



Cite this: *Chem. Commun.*, 2015, 51, 15145

Received 19th June 2015,
Accepted 21st August 2015

DOI: 10.1039/c5cc05064b

www.rsc.org/chemcomm

A one-photon two-electron process was made possible in photocatalytic H₂ evolution from ascorbic acid with a cobalt(II) chlorin complex [Co^{II}(Ch)] via electron transfer from ascorbate to the excited state of [Ru(bpy)₃]²⁺ followed by electron transfer from [Ru(bpy)₃]⁺ to Co^{II}(Ch) with proton to give the hydride complex, which reacts with proton to produce H₂. [Co^{III}(Ch)]⁺ was reduced by ascorbate to reproduce Co^{II}(Ch).

Photocatalytic production of hydrogen (H₂) has attracted increasing attention as a clean energy source because of the ever-increasing demand for energy and climate change on our planet.¹ A number of highly efficient hydrogen evolving systems have been developed including homogeneous and heterogeneous photocatalytic systems.^{2–13} Two electrons are required to produce H₂ from protons, although one photon generates normally only one electron. A mechanism of photocatalytic production of H₂ was reported to clarify how photoinduced electron transfer of a photosensitiser (a one-electron process) leads to H₂ production (a two-electron process).^{14–16} Disproportionation of one-electron reduced species of metal complexes resulted in formation of the two-electron reduced species from which H₂ is formed.¹⁷ Bimolecular reactions of metal(III)-hydride complexes also generate H₂ accompanied by regeneration of metal(II) complexes.¹⁸ In each case, the maximum quantum yield of H₂ production per photon is 50%, because two photons are required to produce two electrons. Thus there has so far been no example for one photon to generate one H₂ molecule.

^a Department of Material and Life Science, Graduate School of Engineering, Osaka University, ALCA and SENTAN, Japan Science and Technology Agency (JST), Suita, Osaka 565-0871, Japan. E-mail: fukuzumi@chem.eng.osaka-u.ac.jp; Fax: +81-6-6879-7370

^b Department of Chemistry and Nano Science, Ewha Womans University, Seoul 120-750, Korea

^c Faculty of Science and Technology, Meijo University, ALCA and SENTAN, Japan Science and Technology Agency (JST), Nagoya, Aichi 468-8502, Japan

† Electronic supplementary information (ESI) available: Experimental details and cyclic voltammograms (Fig. S1), time courses of H₂ evolution (Fig. S2), emission spectra (Fig. S3 and S5), UV-vis absorption spectra (Fig. S4 and S7) and kinetic data (Fig. S6–S11). See DOI: [10.1039/c5cc05064b](https://doi.org/10.1039/c5cc05064b)

Mechanism of a one-photon two-electron process in photocatalytic hydrogen evolution from ascorbic acid with a cobalt chlorin complex†

Shoko Aoi,^a Kentaro Mase,^a Kei Ohkubo^{ab} and Shunichi Fukuzumi^{*abc}

We report herein photocatalytic H₂ evolution from ascorbic acid (AscH₂) with a cobalt(II) chlorin complex [Co^{II}(Ch)] (a chemical structure shown in Scheme 1)¹⁹ in an aqueous acetonitrile solution (H₂O/MeCN), which proceeds *via* a one-photon two-electron process. The photocatalytic mechanism is clarified by nanosecond laser transient absorption spectra and by examining each step in the catalytic cycle independently.

Visible light irradiation of a deaerated (Ar-saturated) H₂O/MeCN solution (1 : 1 v/v) of [Ru(bpy)₃]²⁺ (bpy = 2,2'-bipyridine) containing ascorbic acid (AscH₂) and ascorbate (AscH[–]) ($E_{ox} = 0.43$ V vs. SCE) as an electron donor and Co^{II}(Ch) ($E_{red} = -0.96$ V vs. SCE) (Fig. S1 in the ESI†) as a catalyst resulted in H₂ evolution (Fig. 1, black line). When the ratio of AscH[–] to AscH₂ was changed as fixed total concentrations of AscH₂ and AscH[–] ([AscH₂] + [AscH[–]] = 1.1 M), the largest H₂ evolution activity was attained with AscH[–] (0.30 M) and AscH₂ (0.80 M) (Fig. S2 in ESI†). The smaller concentration of AscH[–] results in less efficient reductive quenching of the [Ru(bpy)₃]^{2+*} emission (* denotes the excited state).

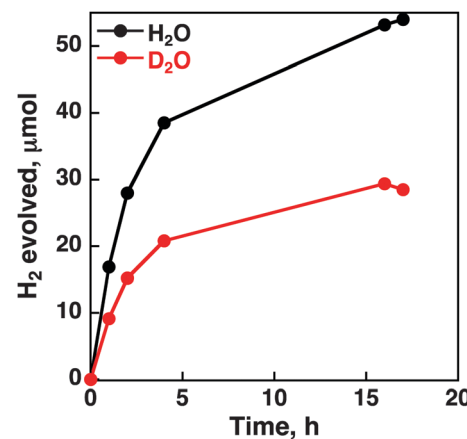


Fig. 1 Time courses of H₂ evolution in the photocatalytic reduction of proton in an Ar-saturated H₂O/MeCN (black) and D₂O/MeCN (red) mixed solution (1 : 1 v/v) containing [Ru^{II}(bpy)₃]²⁺ (2.0 mM), AscH₂ (0.80 M), AscH[–] (0.30 M) and Co^{II}(Ch) (25 μM) under irradiation of visible light ($\lambda > 420$ nm) at 298 K.



The quenching efficiency of $[\text{Ru}(\text{bpy})_3]^{2+*}$ ($E_{\text{red}} = 0.77$ V vs. SCE in MeCN)²⁰ by AsCH^- (0.30 M) with AsCH_2 (0.80 M) was determined to be 95% (Fig. S3 in ESI[†]). On the other hand, the smaller concentration of AsCH_2 may retard H_2 production due to decreasing the acidity. When H_2O was replaced by D_2O , D_2 and HD were produced without formation of H_2 . Thus, hydrogen was produced from water and ascorbic acid as electron and proton sources. The observed deuterium kinetic isotope effect (KIE) in Fig. 1 ($k_{\text{H}}/k_{\text{D}} = 1.8$ in the initial stage) suggests that the Co–H bond cleavage of a cobalt hydride intermediate ($[\text{Co}^{\text{III}}(\text{H})(\text{Ch})]$) by proton may be the rate-determining step for the photocatalytic H_2 evolution (*vide infra*).

The concentration of $\text{Co}^{\text{II}}(\text{Ch})$ was optimised to be 50 μM for the efficient photocatalytic H_2 evolution. The absorption of $[\text{Ru}(\text{bpy})_3]^{2+}$ is blocked by the larger concentration of $\text{Co}^{\text{II}}(\text{Ch})$ (Fig. S4 in ESI[†]).²¹ The quantum yield of the photocatalytic H_2 evolution was determined to be 12% using a ferric oxalate actinometer (see the Experimental section in ESI[†]). This value is similar to the highest value reported for photocatalytic H_2 evolution using a cobalt terpyridine complex ($\Phi = 0.13$).²²

Nanosecond transient absorption spectra of an $\text{H}_2\text{O}/\text{MeCN}$ solution of $[\text{Ru}(\text{bpy})_3]^{2+}$ with AsCH_2 and AsCH^- are shown in Fig. 2, where appearance of the absorption band at 500 nm due to $[\text{Ru}(\text{bpy})_3]^+$ is observed upon the nanosecond laser excitation. Thus, electron transfer from AsCH^- to $[\text{Ru}(\text{bpy})_3]^{2+*}$ occurred to produce AsCH^\bullet and $[\text{Ru}(\text{bpy})_3]^+$. The rate constant of electron transfer from AsCH^- to $[\text{Ru}(\text{bpy})_3]^{2+*}$ (k_{et}) was determined to be $8.0 \times 10^8 \text{ M}^{-1} \text{ s}^{-1}$ from a slope of Stern–Volmer plot ($K_{\text{SV}} = 3.5 \times 10^2 \text{ M}^{-1}$) and the lifetime of $[\text{Ru}(\text{bpy})_3]^{2+*}$ (0.44 μs in water/MeCN 1:1 v/v) (Fig. S5 in ESI[†]).²³ The decay rate of absorbance at 500 nm due to $[\text{Ru}(\text{bpy})_3]^+$ obeyed the second-order kinetics of bimolecular back electron transfer from $[\text{Ru}(\text{bpy})_3]^+$ to AsCH^\bullet . In the presence of $\text{Co}^{\text{II}}(\text{Ch})$, the decay of absorbance became much faster because of electron transfer from $[\text{Ru}(\text{bpy})_3]^+$ to $\text{Co}^{\text{II}}(\text{Ch})$ as shown in Fig. 2b. The decay rate constant linearly increased with increasing the concentration of $[\text{Co}^{\text{II}}(\text{Ch})]$ (Fig. S6 in ESI[†]). The rate constant of electron transfer from $[\text{Ru}(\text{bpy})_3]^+$ to $\text{Co}^{\text{II}}(\text{Ch})$ was determined to be $2.5 \times 10^9 \text{ M}^{-1} \text{ s}^{-1}$ from the slope of dependence of the first-order decay rate constant on concentration of $\text{Co}^{\text{II}}(\text{Ch})$ (Fig. S6b in ESI[†]).

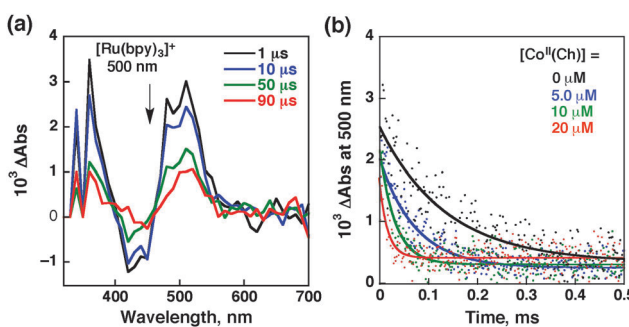


Fig. 2 (a) Transient absorption spectra after laser excitation ($\lambda = 450$ nm) of $[\text{Ru}^{\text{II}}(\text{bpy})_3]^{2+}$ (80 μM) in the presence of AsCH_2 (0.80 M) and AsCHNa (0.30 M) in a deaerated $\text{H}_2\text{O}/\text{MeCN}$ mixed solution (1:1 v/v) at 298 K. (b) Time profiles of absorbance at 500 nm due to decay of $[\text{Ru}(\text{bpy})_3]^+$ in the presence of various concentrations of $\text{Co}^{\text{II}}(\text{Ch})$ (0–20 μM) in deaerated $\text{H}_2\text{O}/\text{MeCN}$ mixed solutions (1:1 v/v) containing $[\text{Ru}^{\text{II}}(\text{bpy})_3]^{2+}$ (80 μM), AsCH_2 (0.80 M), AsCHNa (0.30 M).

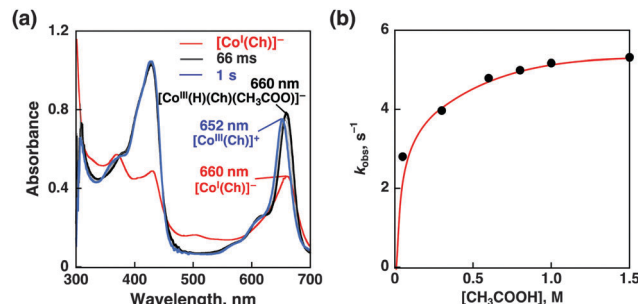
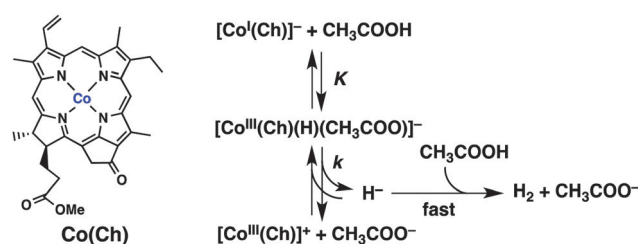


Fig. 3 (a) UV-vis absorption spectral changes of $[\text{Co}^{\text{I}}(\text{Ch})]^-$ (30 μM) upon addition of CH_3COOH (0.30 M) in deaerated MeCN at 298 K. The black and blue lines show the spectra taken at 66 ms and 1 s after mixing, respectively. The red line shows UV-vis absorption spectrum of $[\text{Co}^{\text{I}}(\text{Ch})]^-$ (15 μM) formed by the electron-transfer reduction of $\text{Co}^{\text{II}}(\text{Ch})$ (15 μM) with CoCp_2^* (300 μM) in deaerated MeCN at 298 K. (b) Plot of k_{obs} for the rate of formation of $[\text{Co}^{\text{III}}(\text{Ch})]^+$ vs. $[\text{CH}_3\text{COOH}]$.

To examine the reaction of $[\text{Co}^{\text{I}}(\text{Ch})]^-$ that is produced by electron transfer from $[\text{Ru}(\text{bpy})_3]^+$ to $\text{Co}^{\text{II}}(\text{Ch})$, $[\text{Co}^{\text{I}}(\text{Ch})]^-$ was prepared by the one-electron reduction of $\text{Co}^{\text{II}}(\text{Ch})$ by decamethylcobaltocene $[\text{Co}(\text{Cp}_2^*)_2]$ in MeCN (Fig. S7 in ESI[†]). The UV-vis absorption band of $[\text{Co}^{\text{I}}(\text{Ch})]^-$ (red line in Fig. 3a; $\lambda_{\text{max}} = 510$ nm) decreased with increasing absorption band at 660 nm (black line) at 66 ms after addition of acetic acid (CH_3COOH) (0.30 M). Then, this absorption band was finally blue shifted to $\lambda_{\text{max}} = 652$ nm, which is due to $[\text{Co}^{\text{III}}(\text{Ch})]^+$.^{24,25} Thus, $[\text{Co}^{\text{I}}(\text{Ch})]^-$ may react with CH_3COOH to form the hydride complex ($[\text{Co}^{\text{III}}(\text{H})(\text{CH})(\text{CH}_3\text{COO})]^-$; $\lambda_{\text{max}} = 660$ nm), from which H_2 was evolved by the reaction with CH_3COOH to produce $[\text{Co}^{\text{III}}(\text{Ch})]^+$. The reaction of $[\text{Co}^{\text{I}}(\text{Ch})]^-$ with CH_3COOH was monitored by the absorption change at 652 nm due to $[\text{Co}^{\text{III}}(\text{Ch})]^+$ as shown in Fig. 3, where the rate of the formation of $[\text{Co}^{\text{III}}(\text{Ch})]^+$ obeyed first-order kinetics (Fig. S8 in ESI[†]). The first-order rate constant increased with increasing concentration of CH_3COOH to approach a constant value (Fig. 3b). Such a saturation behaviour indicates that CH_3COOH is not involved in the rate-determining step and that the reaction of $[\text{Co}^{\text{I}}(\text{Ch})]^-$ with CH_3COOH proceeds *via* formation of the hydride complex ($[\text{Co}^{\text{III}}(\text{H})(\text{CH})(\text{CH}_3\text{COO})]^-$), followed by the rate-determining heterolytic cleavage of the $\text{Co}^{\text{III}}\text{–H}$ bond. The subsequent reaction of the released hydride ion with CH_3COOH to produce H_2 and $[\text{Co}^{\text{III}}(\text{Ch})]^+$ may be fast as compared with the back reaction of the $\text{Co}^{\text{III}}\text{–H}$ bond cleavage (Scheme 1). The kinetic equation for the formation of $[\text{Co}^{\text{III}}(\text{Ch})]^+$ is given by eqn (1),



Scheme 1 Mechanism of hydrogen formation by the reaction of $[\text{Co}^{\text{I}}(\text{Ch})]^-$ with CH_3COOH .



$$\frac{d[[\text{Co}^{\text{III}}(\text{Ch})]^+]}{dt} = k[[\text{Co}^{\text{III}}(\text{H})(\text{Ch})(\text{CH}_3\text{COO})]^-] \quad (1)$$

where k is the rate constant of the hydrogen evolution. From the equilibrium constant (K), the concentration of a complex between $[\text{Co}^{\text{I}}(\text{Ch})]^-$ and CH_3COOH is given by eqn (2), where

$$[[\text{Co}^{\text{III}}(\text{H})(\text{Ch})(\text{CH}_3\text{COO})]^-] = K[\text{CH}_3\text{COOH}][[[\text{Co}^{\text{I}}(\text{Ch})]^-]_0 - [[\text{Co}^{\text{III}}(\text{Ch})]^+]/(1 + K[\text{CH}_3\text{COOH}]) \quad (2)$$

$[[\text{Co}^{\text{I}}(\text{Ch})]^-]_0$ is the initial concentration. Eqn (1) is rewritten by eqn (3).

$$\frac{d[[\text{Co}^{\text{III}}(\text{Ch})]^+]}{dt} = kK[\text{CH}_3\text{COOH}][[[\text{Co}^{\text{I}}(\text{Ch})]^-]_0 - [[\text{Co}^{\text{III}}(\text{Ch})]^+]/(1 + K[\text{CH}_3\text{COOH}]) \quad (3)$$

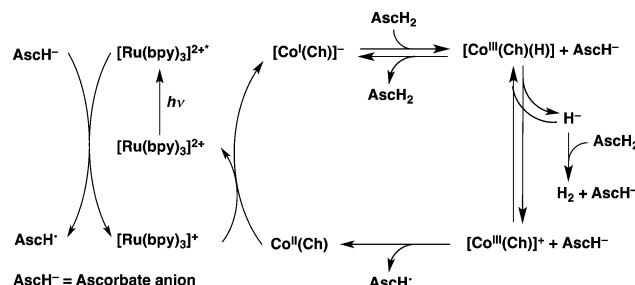
Under the conditions, the concentration of CH_3COOH is much higher than that of $[\text{Co}^{\text{I}}(\text{Ch})]^-$, the k_{obs} value is given by eqn (4). To determine the k value, eqn (4) is rewritten by eqn (5), which predicts

$$k_{\text{obs}} = kK[\text{CH}_3\text{COOH}]/(1 + K[\text{CH}_3\text{COOH}]) \quad (4)$$

$$k_{\text{obs}}^{-1} = 1/kK[\text{CH}_3\text{COOH}]^{-1} + 1/k \quad (5)$$

a linear correlation between k_{obs}^{-1} and $[\text{CH}_3\text{COOH}]^{-1}$ (Fig. S9 in ESI†). The k and K values were determined from the intercept and slope of the linear plot of k_{obs}^{-1} vs. $[\text{CH}_3\text{COOH}]^{-1}$ to be 5.9 s^{-1} and 7.1 M^{-1} .

When CH_3COOH was replaced by CH_3COOD , the deuterium kinetic isotope effect (KIE) was observed (Fig. S10 in ESI†),²⁶ indicating that the cleavage of the Co-H bond of $[\text{Co}^{\text{III}}(\text{H})(\text{Ch})(\text{CH}_3\text{COO})]^-$ or O-H bond of CH_3COOH is involved in the rate-determining step of the reaction of $[\text{Co}^{\text{I}}(\text{Ch})]^-$ with CH_3COOH . Because CH_3COOH is not involved in the rate-determining step (*vide infra*), the cleavage of the Co-H bond of $[\text{Co}^{\text{III}}(\text{H})(\text{Ch})(\text{CH}_3\text{COO})]^-$ is the rate-determining step of the reaction of $[\text{Co}^{\text{I}}(\text{Ch})]^-$ with CH_3COOH . The KIE value was 1.7 which is virtually the same as observed for the photocatalytic H_2 evolution (KIE = 1.8, Fig. 1), indicating that the heterolytic Co-H bond cleavage of $[\text{Co}^{\text{III}}(\text{H})(\text{Ch})(\text{CH}_3\text{COO})]^-$ is also the rate-determining step in the photocatalytic H_2 evolution.



Scheme 2 Mechanism of photocatalytic hydrogen evolution from Asch^- and Asch_2 with $[\text{Ru}(\text{bpy})_3]^{2+}$ and $\text{Co}^{\text{II}}(\text{Ch})$.

$[\text{Co}^{\text{III}}(\text{Ch})]^+$ produced by the reaction of $[\text{Co}^{\text{III}}(\text{H})(\text{Ch})(\text{CH}_3\text{COO})]^-$ with CH_3COOH is reduced by Asch^- to form $\text{Co}^{\text{II}}(\text{Ch})$ as shown by stopped-flow measurements in Fig. 4.²⁷ The rate constant of electron transfer from Asch^- to $[\text{Co}^{\text{III}}(\text{Ch})]^+$ that was prepared by the one-electron oxidation of $\text{Co}^{\text{II}}(\text{Ch})$ with $(p\text{-BrC}_6\text{H}_4)_3\text{N}^+\text{SbCl}_6^-$ in $\text{H}_2\text{O}/\text{MeCN}$ was determined to be $1.5 \times 10^3 \text{ M}^{-1} \text{ s}^{-1}$ from the linear dependence of the first-order rate constant on concentration of Asch^- (Fig. S11 in ESI†).

The photocatalytic cycle is summarized in Scheme 2. Photoexcitation of $[\text{Ru}(\text{bpy})_3]^{2+}$ resulted in electron transfer from Asch^- to $[\text{Ru}(\text{bpy})_3]^{2+*}$ to produce $[\text{Ru}(\text{bpy})_3]^{+}$, followed by electron transfer from $[\text{Ru}(\text{bpy})_3]^{+}$ to $\text{Co}^{\text{II}}(\text{Ch})$ to produce $[\text{Co}^{\text{I}}(\text{Ch})]^-$, which reacts with Asch_2 to produce $[\text{Co}^{\text{III}}(\text{H})(\text{Ch})(\text{Asch})]^-$. Hydrogen is generated by the reaction of $[\text{Co}^{\text{III}}(\text{H})(\text{Ch})(\text{Asch})]^-$ with Asch_2 via the Co-H bond heterolysis to produce $[\text{Co}^{\text{III}}(\text{Ch})]^+$,^{28,29} which is reduced by Asch^- to regenerate $\text{Co}^{\text{II}}(\text{Ch})$. In such a case, a one-photon two-electron process is made possible, because one photon is required to produce $[\text{Co}^{\text{I}}(\text{Ch})]^-$ for H_2 evolution and another electron is provided thermally by Asch^- .

In conclusion, $\text{Co}^{\text{II}}(\text{Ch})$ acts as an efficient catalyst for photocatalytic H_2 evolution from ascorbic acid with $[\text{Ru}(\text{bpy})_3]^{2+}$ as a photocatalyst to attain the high quantum yield via a one-photon two-electron process in which the second electron is provided thermally from ascorbic acid.

This work was supported by Grants-in-Aid (no. 26620154 and 26288037 to K.O.) and JSPS fellowship (No. 25-727 to K.M.) from the Ministry of Education, Culture, Sports, Science and Technology (MEXT); ALCA and SENTAN projects from JST, Japan (to S.F.).

Notes and references

- R. A. Kerr and R. F. Service, *Science*, 2005, **309**, 101.
- X. Song, H. Wen, C. Ma, H. Chen and C. Chen, *New J. Chem.*, 2015, **39**, 1734.
- K. Kawano, K. Yamauchi and K. Sakai, *Chem. Commun.*, 2014, **50**, 9872.
- X. Wang, S. Goeb, Z. Ji, N. A. Pogulaichenko and F. N. Castellano, *Inorg. Chem.*, 2011, **50**, 705.
- L.-Z. Fu, L.-L. Zhou, L.-Z. Tang, Y.-X. Xhang and S.-Z. Zhan, *J. Power Sources*, 2015, **280**, 453.
- S. Fukuzumi, *Curr. Opin. Chem. Biol.*, 2015, **25**, 18.
- D. Basu, S. Mazumder, X. Shi, H. Baydoun, J. Niklas, O. Poluektov, H. B. Schlegel and C. N. Verani, *Angew. Chem., Int. Ed.*, 2015, **54**, 2105.
- A. Call, Z. Codola, F. Acuna-Pares and J. Lloret-Fillol, *Chem. - Eur. J.*, 2014, **20**, 6171.
- H. Lv, W. Guo, K. Wu, Z. Chen, J. Bacsá, D. G. Musaev, Y. V. Geletii, S. M. Lauinger, T. Lian and C. L. Hill, *J. Am. Chem. Soc.*, 2014, **136**, 14015.

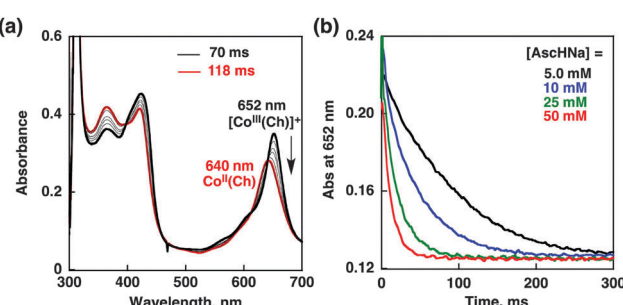


Fig. 4 (a) UV-vis absorption spectral changes in the electron-transfer reduction of $[\text{Co}^{\text{III}}(\text{Ch})]^+$ ($15 \mu\text{M}$) with AscHNA (50 mM) in air-saturated $\text{H}_2\text{O}/\text{MeCN}$ mixed solutions ($1:1 \text{ v/v}$) at 298 K taken at 70 ms and 118 ms after mixing. (b) Decay time profiles of absorbance at 652 nm due to $[\text{Co}^{\text{III}}(\text{Ch})]^+$ in the presence of various concentrations of AscHNA in air-saturated $\text{H}_2\text{O}/\text{MeCN}$ mixed solutions ($1:1 \text{ v/v}$) at 298 K .



10 L. Chen, G. Chen, C.-F. Leung, S.-M. Yiu, C.-C. Ko, E. Anxolabéhère-Mallart, M. Robert and T.-C. Lau, *ACS Catal.*, 2015, **5**, 356.

11 A. Zarkadoulas, E. Koutsouri, C. Kefalidi and C. A. Mitsopoulou, *Coord. Chem. Rev.*, 2014, **11**, 6.

12 K. Maeda, M. Eguchi and T. Oshima, *Angew. Chem., Int. Ed.*, 2014, **53**, 13164.

13 J. Zhao, Y. Ding, J. Wei, X. Du, Y. Yu and R. Han, *Int. J. Hydrogen Energy*, 2014, **39**, 18908.

14 E. Deponti, A. Luisa, M. Natali, E. lengo and F. Scandola, *Dalton Trans.*, 2014, **43**, 16345.

15 H. Ozawa and K. Sakai, *Chem. Commun.*, 2011, **47**, 2227.

16 A. Rodenberg, M. Orazielli, B. Probst, C. Bachmann, R. Alberto, K. K. Baldridge and P. Hamm, *Inorg. Chem.*, 2015, **54**, 646.

17 S. Fukuzumi, T. Kobayashi and T. Suenobu, *Angew. Chem., Int. Ed.*, 2011, **50**, 728.

18 J. L. Dempsey, B. S. Brunschwig, J. R. Winkler and H. B. Gray, *Acc. Chem. Res.*, 2009, **42**, 1995.

19 K. Mase, K. Ohkubo and S. Fukuzumi, *J. Am. Chem. Soc.*, 2013, **135**, 2800.

20 J. Yuasa and S. Fukuzumi, *J. Am. Chem. Soc.*, 2006, **128**, 14281.

21 The photocatalytic H_2 evolution in our optimized conditions, the absorption at $\lambda = 450$ nm of $[Ru(bpy)_3]^{2+}$ (2.0 mM, $\epsilon_{450nm} = 1.4 \times 10^4 \text{ M}^{-1} \text{ cm}^{-1}$) is not significantly blocked by that of $Co^{II}(Ch)$ ($Abs_{450nm} = 0.38$; $\epsilon_{450nm} = 1.8 \times 10^4 \text{ M}^{-1} \text{ cm}^{-1}$) under this experimental conditions.

22 C. V. Krishnan and N. Sutin, *J. Am. Chem. Soc.*, 1981, **103**, 2141.

23 The emission lifetime of $[Ru(bpy)_3]^{2+*}$ in water at 298 K was reported to be 0.58 μs ; see: J. V. Houten and R. J. Watts, *J. Am. Chem. Soc.*, 1976, **98**, 4853.

24 The spectrum of $[Co^{III}(Ch)]^+$ obtained by the reaction $[Co^I(Ch)]^-$ with CH_3COOH was identical to that of $[Co^{III}(Ch)]^+$ prepared by the electron-transfer oxidation of $Co^{II}(Ch)$ by a one-electron oxidizing reagent of $(p-BrC_6H_4)_3N^{+}SbCl_6^-$ ($E_{red} = 1.05 \text{ V vs. SCE}$).¹⁹

25 $[Co^{III}(Ch)]^+$ or $Co^{III}(H)(Ch)$ species is not re-reduced by large excess of $Co(Cp^*)_2$, under the present reaction conditions because $Co^{II}(Ch)$ with 20 molar equiv. of $Co(Cp^*)_2$ is necessary to quantitatively produce $[Co^I(Ch)]^-$ as shown in ESI,[†] Fig. S7. $Co(Cp^*)_2$ ($E_{1/2}^{+/-} = -1.47 \text{ V vs. SCE}$) is unstable even in carefully degassed and dehydrated MeCN.

26 The KIE value was determined from the k_{obs} values at $[CH_3COOH] = [CH_3COOD] = 1.0 \text{ M}$.

27 Neither oxidation of $[Co^{III}(Ch)]^+$ nor O_2 reduction was observed under the basic reaction conditions.

28 S. Mandal, S. Shikano, Y. Yamada, Y.-M. Lee, W. Nam, A. Llobet and S. Fukuzumi, *J. Am. Chem. Soc.*, 2013, **135**, 15294.

29 No $Co(n)-H$ complex is involved in the heterolysis of the Co–H bond as reported in ref. 28.

